A Multispectral Canopy LiDAR Demonstrator Project

Iain H. Woodhouse, Caroline Nichol, Peter Sinclair, Jim Jack, Felix Morsdorf, Tim J. Malthus, and Genevieve Patenaude

***Abstract*—The first demonstration of a multispectral light detection and ranging (LiDAR) optimized for detailed structure and physiology measurements in forest ecosystems is described. The basic principle is to utilize, in a single instrument, both the capacity of multispectral sensing to measure plant physiology [through normalized difference vegetation index (NDVI) and photochemical reflectance index (PRI)] with the ability of LiDAR to measure vertical structure information and generate "hot spot" (specular) reflectance data independent of solar illumination. A tunable laser operated at four wavelengths (531, 550, 660, and 780 nm) was used to measure profiles of the NDVI and the PRI. Laboratory-based measurements were conducted for live trees, demonstrating that realistic values of the indexes can be measured. A model-based analysis demonstrates that the LiDAR waveforms cannot only capture the tree height information but also picks up the seasonal and vertical variation of NDVI inside the tree canopy.**

***Index Terms*—Forest canopy, multispectral light detection and ranging (LiDAR), normalized difference vegetation index (NDVI).**

I. Introduction and Concept

IN THIS letter, we describe the development and testing of a new multispectral light detection and ranging (LiDAR) that has been optimized to measure key variables of a forest canopy. For a decade, LiDAR has been used to retrieve forest parameters such as tree height, crown diameter, number of stems, stem diameter, and basal area [1]. LiDAR remote sensing has been also widely used to infer estimates of vegetation structure and biomass [2]–[4] at various scales, i.e., ranging from a single-tree level [5] to a landscape level. The novelty of the LiDAR described here is that it measures the profile of reflectance at four wavelengths (531, 550, 690, and 780 nm) chosen so that the photochemical reflectance index (PRI) and the normalized difference vegetation index (NDVI) can be measured through a canopy, in addition to the usual LiDAR parameters. This is not possible with any other current LiDAR system.

The development of the concept, and instrument, has been based on more than three decades of successful measurements over a variety of forested ecosystems by passive multispectral sensors and the maturing technologies of single wavelength LiDAR that can now provide detailed vertical structure from airborne platforms. LiDAR that actively measure vegetation spectral response, in well-chosen narrow wavelength bands will provide unprecedented information, both as a detailed sampling tool and for calibration of passively acquired multispectral data.

Manuscript received June 23, 2009; revised November 10, 2009 and June 10, 2010; accepted July 15, 2010. Date of publication April 21, 2011; date of current version August 26, 2011. This work was supported by the Natural Environment Research Council Centre for Earth Instrumentation as a Seed-Corn Project.

I. H. Woodhouse, C. Nichol, T. J. Malthus, and G. Patenaude are with the School of GeoSciences, University of Edinburgh, EH8 9XP Edinburgh, U.K. (e-mail: i.h.woodhouse@ed.ac.uk).

P. Sinclair and J. Jack are with SELEX Galileo, EH5 2XS Edinburgh, U.K.

F. Morsdorf is with the University of Zurich, 8006 Zurich, Switzerland.

Color versions of one or more of the figures in this paper are available online at http://ieeexplore.ieee.org.

Digital Object Identifier 10.1109/LGRS.2011.2113312

II. Background and Need for Measurements

The value of a multispectral canopy LiDAR (MSCL) is that it combines the advantages of multispectral reflectance with the vertical profile capabilities of LiDAR. In vegetation and land cover studies, more than 30 years of space-borne multispectral data have been recognized for their following abilities to: 1) map species composition; 2) discriminate and identify healthy versus stressed canopies; 3) provide information on the photosynthetic capabilities of plants (fPAR); and 4) provide a diagnostic of a range of plant physiological properties and processes through the mapping of pigment concentrations dynamics.

Pioneering research at The University of Edinburgh has demonstrated the utility of narrow waveband (hyperspectral and passive) reflectance indexes for assessing canopy photosynthetic light use efficiency ε of vegetation, which is a key parameter required for the calculation of carbon uptake of vegetation [6], [7]. The biophysical basis of this is well established: When excess light is absorbed by chlorophyll, the ε falls, and the relative proportions of a set of accessory pigments (xanthophylls) change, causing a measurable change in both ε and the reflectance centered at 531 nm. This change can be measured with high-resolution spectroradiometry and incorporated into a spectral index (using a reference waveband at 550 nm) called PRI. This allows for the remote measurement of ε over whole landscapes [8]. All canopy PRI work to date has been carried out with passive optical sensors, and this is the first study to use active system (i.e., laser approach). With this in mind, the wavelengths of 531 and 550 nm were chosen as two of the four laser wavelengths. The other two wavelengths selected were at 690 and 780 nm and therefore located on either side of the red edge to estimate NDVI, allowing discrimination of woody and nonwoody vegetation.

While passive optical data alone cannot detect processes inside or in the lower parts of the canopy, a multispectral LiDAR system has the capacity to overcome this limitation. Additionally, such a system has the following benefits: 1) high reflectivity provided by monostatic active sensing, with no shadowing (the high specular return observed at the "hot spot") and no dependence on solar illumination conditions, other than as a background signal; 2) precise pointing capability with narrow laser beamwidth that allows the kinds of high spatial resolution expected of multispectral sensors (and thus minimizes "mixed-pixel" effects); 3) removal of along-path reflectance from atmospheric aerosols by careful wavelength selection to improve confidence in target spectral reflectance; 4) vertical signal discrimination allowing differentiation of overstorey and understorey, spectral distribution of canopy density, and gap

properties [9]; 5) ability to quantify canopy height [10], terrain elevation [11] and, indirectly, tree biomass and carbon [2]; and 6) the ability to discriminate between species based on foliage spectral profiles [12].

The synergetic potential of LiDAR with multispectral and hyperspectral sensors for vegetation studies has been tested and demonstrated (via the combination of hyperspectral instrument data and LiDAR instrument data) [4], [12], [13], further iterating the potential for a single instrument that integrates the advantages of both approaches (e.g., [14]). In so doing, it is a more compact instrument than a combined LiDAR/imager primarily designed for bio study. Such simultaneous measurements by the same instrument enable more reliable measurements of the four carefully selected frequencies so that we can characterize the main properties of trees, e.g., height, PRI, NDVI, and crown size (dependent on high sampling).

Most works to date on forests have been through the fusion of multispectral imagery with standard profiling LiDAR. The instrument described here differs from previous LiDAR sensors in that it has four wavelengths optimized for two vegetation indexes. A previous work has focused on two wavelengths, usually for measuring only NDVI [15] or no particular vegetation index [16], [17]. In [18], a generic multispectral system is described but not optimized for vegetation. Using LiDAR to induce a fluorescence response has been also described, but this does not provide information on vertical structure [19].

III. Instrument Description

The principles of a canopy LiDAR are well established. A laser pulse is emitted and travels to the ground where it is reflected from the ground or partially reflected by intercepting the upper vegetation canopy or intermediate branches. The reflected energy is measured using a receiver in the LiDAR that can discriminate the different returns. The returned signals, together with the platform position, is recorded for storage or further processing. A multispectral system can emit simultaneous or sequential pulses at the different wavelengths.

The (two-way) time of flight is proportional to the range and to the target, and the return signal intensity will depend on the reflectance of the ground material and the proportion of the beam intercepted. The intensity will also depend on the laser pulse wavelength. Fast and accurate digitization of the return signal captures and records the information for postprocessing. The instrument thus provides a measure of the vegetation structure or density and the reflectivity as a function of height within the vegetation at different wavelengths.

A. Components

The MSCL described here was developed and built by SELEX Galileo under its standard procedures for a demonstrator equipment suitable for field trials. Its SELEX Part Number is CT02028-002. The design was approved through a SELEX Preliminary and Critical Design Review. A block diagram illustrating the main components is shown in Fig. 1(a). The laser is a commercially available integrated tunable laser system, which consists of a Nd:YAG pump laser, wavelength conversion modules, and accessories. The raw output pulse energies can exceed 1 mJ per pulse over the selected wavelengths. For the short-range experiments reported here, the laser energy has been reduced by using neutral density (ND) filters in the laser

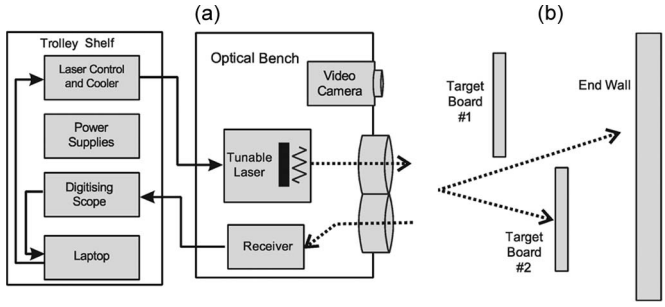

Fig. 1. Block diagram illustrating (a) the LiDAR breadboard and (b) the testing setup.

exit path. The pulsewidth is ∼5 ns over the wavelength range. The polarization is linear. A pulse repetition frequency of 20 Hz was used. For detection, an integrated module with silicon photodiode and integrated amplifier was used. The module has a bandwith of 1 GHz and a low noise level. A digitizing oscilloscope at 5 gigasamples/s and 8-bit digitization was used.

B. LiDAR Features

A tunable pulsed laser source was chosen, as opposed to fixed wavelength laser sources, as this would allow further experiments of the wavelength-dependent backscatter of foliage. A consequence of this is that the required laser wavelengths are not simultaneously available, but the laser is rapidly retuned to alternative wavelengths. The tuning range extends from visible into the shortwave infrared. The unmodified laser output is linearly polarized and forms an elliptical beam shape. Narrow laser pulses, which are an advantage in resolution and peak signal, are generated. The pulsewidth is 4.75 ns. To represent the return signal accurately, the receiver is required to have a very fast response time. In this instrument, the "state-of-the-art" receiver has very high frequency bandwidth and low noise necessary to provide this response time. The return energy is focused by optics onto the receiver and a high fidelity analog signal is produced. This is then digitized for storage and processing.

C. Calibration

In principle, all the qualities of the LiDAR range equation, except for the vegetation reflectance, are known, allowing vegetation reflectance to be calculated for any LiDAR observation. In practice, these quantities are wavelength dependent, which makes an accurate measurement more difficult.

An alternative used here is to measure the receiver voltage from a reference material surface, at each wavelength. Then, all the remaining parameters in the range equation are equal and cancel leaving, i.e.,

$$\rho_{\mathrm{veg}} = \rho_{\mathrm{ref}} V_{\mathrm{veg}} / V_{\mathrm{ref}} \tag{1}$$

where ρ_{veg} is the vegetation reflectance, ρ_{ref} is the reference material reflectance, V_{veg} is the receiver voltage, as measured from the vegetation, and V_{ref} is the receiver voltage, as measured from the reference material. This technique can be also used in airborne systems where the instrument can be calibrated in this manner prior to flight and can be flown over known reflectivity materials.

D. LiDAR Testing

Testing of the assembled LiDAR was performed at various levels including the following.

1) Test and characterization of the laser only: This was used to characterize the laser and confirm energy values and beam and pulse parameters.
2) Test and characterization of the LiDAR in specialist laser laboratory: Here, the overall LiDAR functions were tested including introducing target boards intercepting the laser beam to check range returns.

These measurements show that a range resolution of < 0.5 m has been demonstrated for this setup and that multiple returns can be detected and digitized. For operational use, we would consider reducing the pulselength to improve the range resolution. Measurements of laser output energy and measured receiver voltage were shown to be stable and provide a reflectance measurement relative to a reference of better than 10%. The range measurements were referenced to an electrical signal indicating that the laser had been commanded to fire. Due to the design of the laser, there was a delay between this signal and the transmission of the laser pulse. This delay only depends on the wavelength selected and was stable. It was therefore possible to measure the delay and compensate for this in the analysis of the reflectivity with range.

E. LiDAR Foliage Measurements

The LiDAR was tested in the laboratory where tests with live trees were conducted in a controlled environment. Two healthy potted conifer trees were used as representative samples. A horizontal measurement setup was used, by tilting the trees, and a panel board was used as a backstop, approximately 1.6 m from the lowest branch. The SELEX laboratory was used to provide representative field trial distances (ranges) to the samples of approximately 23 m. The LiDAR is approved for use in field trials subject to an appropriate site being used and that health and safety provisions can be met.

Fig. 2 shows the digitized LiDAR returns from Tree 1. The amplitude values were calibrated as per Section III-C but with the units arbitrarily scaled. The results are now corrected for pulse time delays. This was achieved by fitting Gaussians to the original pulse in the recorded signal and by determining the horizontal difference of their centroids. A series of individual samples were averaged to reduce noise, and this is described in Section IV-B.

Note that the interval between the vegetation return and the backstop return was measured to be approximately 1.6 m, corresponding to the experimental arrangement. Additionally, the LiDAR laser spot was arranged toward the vegetation edge to guarantee penetration through the foliage to the target behind.

IV. LiDAR Measurements and Observations

A. Laser Pulse Delay

Timing measurement signals are synchronized to an electrical pulse "trigger signal" generated by the first stage of the laser, i.e., the pump laser. The output wavelengths are generated in an optical parametric oscillator (OPO). The output optical pulses of the OPO are generated within the envelope of the optical pump pulses from the pump laser. At the shorter output wavelengths, the OPO is operating further above threshold,

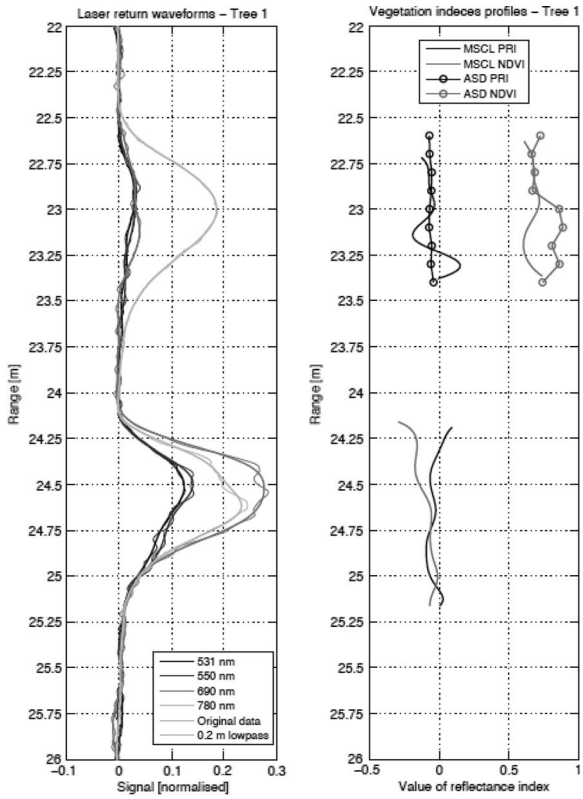

Fig. 2. (Left panel) Laboratory measured LiDAR return. (Left-hand panel) The profiles of PRI and NDVI measured by the LiDAR in the laboratory, with the profiles of PRI and NDVI measured using a portable hyperspectral radiometer superimposed. The lower half of the graph where the PRI and NDVI are similar is the LiDAR return of the calibrated panels behind the target tree.

generating higher energy pulses that appear earlier under the envelope of the optical pump pulse. Therefore, relative to a trigger signal from the pump laser, a shorter wavelength OPO output appears sooner than a longer wavelength output. The time delay appears as a small range difference of approximately 0.3 m, but since this is a fixed delay, it can be measured and a correction applied. The range correction is easily corrected, but an alternative is to measure the output pulse directly, leaving the LiDAR by means of a pick-off of the energy such as a small-diameter optical fiber.

B. Receiver Noise Pickup

It was apparent from uncalibrated outputs that there existed some residual level of noise on the digitized receiver outputs. Closer inspection showed evidence of high-frequency pickup or "ringing" on the receiver output. In practice, this is not unexpected as the equipment at this stage was not electrically optimized. A hardware review would measure grounding (earth) paths and presence of ground loops and where applicable would add cable screening (twisted pairs) and filtering (ferrite modules).

In addition, the instrument is also currently operating with large ND attenuation of the laser; this is precautionary for initial characterization, and it reduces laser-eye hazards. As a result, the instrument is operating at a low-signal level. Following these sets of measurements, the signal can be significantly increased, which, of course, improves the signal to noise levels and allows measurements at greater distances. Sample averaging was used at this stage to reduce the apparent noise.

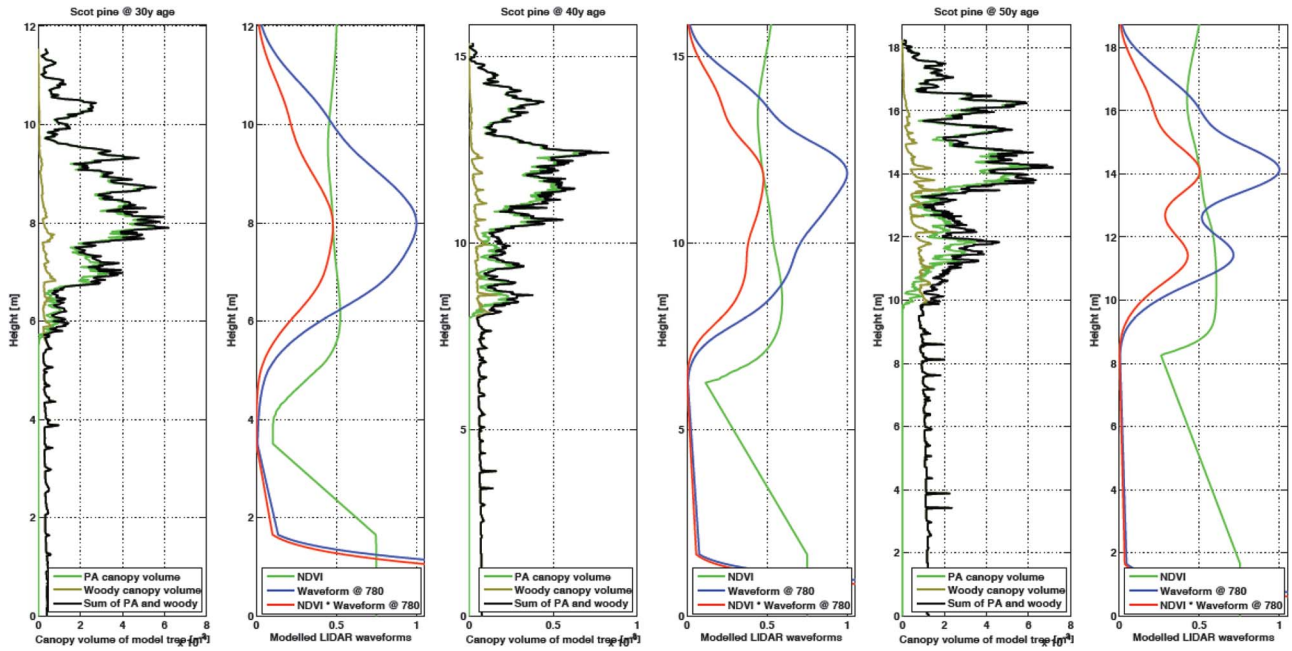

Fig. 3. Canopy volume profiles and simulated LiDAR waveforms for trees of 30, 40, and 50 years of age. (Right panels) Photosynthetic active and woody volume components. (Left panels) Backscatter at 780 nm.

C. Laser Power Output

The laser was selected as the best compromise for this phase of development. In particular, it has very wide wavelength tunability and acceptable laser pulsewidth. Future technology would use an optimized laser source where laser diodes would be used. This allows the following:

1) operation at higher pulse repetition frequency;
2) pulse timing and energy stability to be improved;
3) potential to reduce pulsewidths;
4) increased operating lifetime and reliability.

We also carried out a series of measurements with a passive hyperspectral radiometer on the (same) trees used for the laboratory measurements with the LiDAR. The objective of this endeavor was to generate profiled values of PRI and NDVI to compare with the continuous PRI and NDVI profiles from the LiDAR. An ASD Fieldspec Pro (Analytical Spectral Devices, Boulder, CO, USA: 350–2500 nm; full width at half maximum (FWHM) of 1.4, 350–1050, and 10 nm from 1050 to 2500 nm) fitted with a contact probe was used for shoot-level measurements of reflectance. Multiple single scans were taken at each sampling point and normalized to reflectance using the radiance of a calibrated white target (Spectralon).

The passive reflectance data were then averaged to each sampling point $(n = 6)$ and standard deviations calculated. Plots of profile PRI and NDVI can be found in Fig. 2, with the profile of PRI and NDVI as measured by the LiDAR alongside. The profile of PRI is flat and marginally negative throughout the vertical (compared to the calibration target), which is expected given the lack of notable stress that the tree would have been experiencing. The NDVI profile is similar in value to the LiDAR measured profile (between 0.6–0.8).

V. LiDAR Modeling Approach

The modeling approach used to simulate LiDAR return waveforms in this letter consists of three different models, i.e., one each for the leaf optical properties, the tree structure, and the LiDAR measurement process. An in depth description of the modeling is described in [20], where a widely used model of leaf optical properties [21] was utilized to compute reflectance and transmission values of leaf tissue at the proposed MSCL wavelengths. We used the TREEGROW model [22] to produce structurally sound representations of Scots pine trees at different ages (see [23] and [24] for details).

The gained reflectance and transmittance values were then assigned to the cylinder class in the TREEGROW output representing shoots. For bark and twigs, the measured spectra of pine trees were used, as in [25]. The modeling builds upon the open-source ray-tracing program, i.e., Persistence of Vision Raytracer, whose scene and light descriptions were adapted to represent the LiDAR measurement process.

In Fig. 3, three modeled waveforms for 30-, 40-, and 50-year-old trees are plotted side by side with a "real" canopy volume computed from the model tree. It was possible to differentiate between photosynthetically active canopy volume (shoots) and woody material volume (twigs and branches) in the tree model. The modeled waveforms exhibit the same vertical structure for all four wavelengths but have different amplitudes. For this reason (and to save space), we present only the 780-nm waveform in Fig. 3. From those waveforms, the most striking effect is the amount of smoothing due to the rather long laser pulse of 1.43 m at FWHM used in the modeling; all vertical features in the canopy volume profile smaller than this distance are smoothed out. A second feature of the return waveform is an apparent increase in tree height as well due to the convolution with the laser pulse, which makes the trees appear about 0.75–1 m taller in the return waveform. A regression (not shown here) of LiDAR derived heights with the real heights of the model trees resulted in an R^2 of 0.99, with a mean overestimation of model tree height by LiDAR by about 0.7 m. A remedy to this with a real LiDAR system would be to know the length and the shape of the transmitted pulse.

These results demonstrate that height information can be accurately retrieved from the modeled waveforms. However, we were also interested in assessing the physiological information content of a multiple wavelength LiDAR system. Since two of the modeled bands are enclosing the red edge (the sharp increase in reflectance/transmittance between 660 and 780 nm), we are capable of computing an NDVI profile for the modeled trees according to the following equation. This spectral band ratio is depicted as a green line in the right panels of Fig. 3. It was not possible to model PRI due to the lack of sufficient narrow-bandwidth reflectivity information.

The model results also demonstrate that it is possible to use this methodology to monitor seasonal fluctuations of NDVI. However, the observed seasonal NDVI signal was smaller than the vertical variation inside the tree crown.

VI. Conclusion and Outlook

This letter has described a ground breaking project to demonstrate the feasibility of an MSCL for detailed structure and physiology measurements in forest ecosystems. The project has designed and constructed a prototype breadboard demonstrator instrument. The MSCL concept was submitted as a patent application (No. 0808340.4). The basic principle is to combine in one instrument the proven strengths of passive multispectral sensing to measure plant physiology (through the NDVI and PRI indexes) with the ability of LiDAR systems to measure vertical structure information. Such an instrument is potentially superior to the use of single-wavelength LiDAR systems combined with passive multispectral data since it generates "hot spot" reflectance data, independent of solar illumination, penetrating to otherwise shaded regions of the canopy understory, as well as providing the ability to separate canopy from ground returns. The ability to conduct such measurements will allow better mapping of forest structure and processes that are directly related to photosynthesis and will therefore significantly improve our ability to measure and map the terrestrial biosphere and understand the carbon cycle, land cover use, and biodiversity. Although not fully optimized, the instrument did allow for realistic values of the indexes to be measured.

In parallel to the laboratory measurements, we have also conducted a model-based analysis. It has been shown that the LiDAR waveforms would not only capture the tree height information but as would also pick up the seasonal and vertical variation of the NDVI computed from two of the four MSCL wavelengths inside the tree canopy. A new multiwavelength LiDAR predictor variable could significantly improve the retrieval accuracy of photosynthetically active biomass, as opposed to using a single wavelength LiDAR alone. It remains unclear, however, if these findings would persist for entire forest stands, and further modeling requires to be done to determine this.

References

[1] J. Hyyppa, H. Hyyppa, D. Leckie, F. Gougeon, X. Yu, and M. Maltamo, "Review of methods of small-footprint airborne laser scanning for extracting forest inventory data in boreal forests," *Int. J. Remote Sens.*, vol. 29, no. 5, pp. 1339–1366, Mar. 2008.

[2] G. Patenaude, R. A. Hill, R. Milne, D. L. A. Gaveau, B. B. J. Briggs, and T. P. Dawson, "Quantifying forest above ground carbon content using LiDAR remote sensing," *Remote Sens. Environ.*, vol. 93, no. 3, pp. 368–380, Nov. 2004.

[3] K. S. Lim and P. M. Treitz, "Estimation of above ground forest biomass from airborne discrete return laser scanner data using canopy-based quantile estimators," *Scand. J. Forest Res.*, vol. 19, no. 6, pp. 558–570, Dec. 2004.

[4] P. Hyde, R. Dubayah, W. Walker, J. B. Blair, M. Hofton, and C. Hunsaker, "Mapping forest structure for wildlife habitat analysis using multi-sensor (LiDAR, SAR/InSAR, ETM plus, Quickbird) synergy," *Remote Sens. Environ.*, vol. 102, no. 1/2, pp. 63–73, May 2006.

[5] F. Morsdorf, E. Meier, B. Kotz, K. I. Itten, M. Dobbertin, and B. Allgower, "LIDAR-based geometric reconstruction of boreal type forest stands at single tree level for forest and wildland fire management," *Remote Sens. Environ.*, vol. 92, no. 3, pp. 353–362, Aug. 2004.

[6] C. J. Nichol, K. F. Huemmrich, T. A. Black, P. G. Jarvis, C. L. Walthall, J. Grace, and F. G. Hall, "Remote sensing of photosynthetic-light-use efficiency of boreal forest," *Agricultural Forest Meteorol.*, vol. 101, no. 2/3, pp. 131–142, Mar. 2000.

[7] C. J. Nichol, J. Lloyd, O. Shibistova, A. Arneth, C. Roser, A. Knohl, S. Matsubara, and J. Grace, "Remote sensing of photosynthetic-light-use efficiency of a Siberian boreal forest," *Tellus B, Chem. Phys. Meteorol.*, vol. 54, no. 5, pp. 677–687, Nov. 2002.

[8] J. A. Gamon, L. Serrano, and J. S. Surfus, "The photochemical reflectance index: An optical indicator of photosynthetic radiation use efficiency across species, functional types, and nutrient levels," *Oecologia*, vol. 112, no. 4, pp. 492–501, 1997.

[9] F. Morsdorf, B. Kotz, E. Meier, K. I. Itten, and B. Allgower, "Estimation of LAI and fractional cover from small footprint airborne laser scanning data based on gap fraction," *Remote Sens. Environ.*, vol. 104, no. 1, pp. 50–61, Sep. 2006.

[10] C. Hopkinson, L. Chasmer, K. Lim, P. Treitz, and I. Creed, "Towards a universal LiDAR canopy height indicator," *Can. J. Remote Sens.*, vol. 32, no. 2, pp. 139–152, 2006.

[11] C. Carabajal and D. Harding, "SRTM C-band and ICESat laser altimetry elevation comparisons as a function of tree cover and relief," *Photogramm. Eng. Remote Sens.*, vol. 72, no. 3, pp. 287–298, Mar. 2006.

[12] V. Thomas, D. A. Finch, J. H. McCaughey, T. Noland, L. Rich, and P. Treitz, "Spatial modelling of the fraction of photosynthetically active radiation absorbed by a boreal mixedwood forest using a LiDAR-hyperspectral approach," *Agricultural Forest Meteorol.*, vol. 140, no. 1–4, pp. 287–307, 2006.

[13] J. Mundt, D. Streutker, and N. Glenn, "Mapping sagebrush distribution using fusion of hyperspectral and LiDAR classifications," *Photogramm. Eng. Remote Sens.*, vol. 72, no. 1, pp. 47–54, Jan. 2006.

[14] B. Koetz, G. Q. Sun, F. Morsdorf, K. J. Ranson, M. Kneubuhler, K. Itten, and B. Allgower, "Fusion of imaging spectrometer and LIDAR data over combined radiative transfer models for forest canopy characterization," *Remote Sens. Environ.*, vol. 106, no. 4, pp. 449–459, Feb. 2007.

[15] J. A. R. Rall and R. G. Knox, "Spectral ratio biospheric LiDAR," in *Proc. 22nd ILRC*, 2004, vol. 1, 2, and 561, pp. 831–834.

[16] S. Tan and R. Narayanan, "Design and performance of a multiwavelength airborne polarimetric Lidar for vegetation remote sensing," *Appl. Opt.*, vol. 43, no. 11, pp. 2360–2368, Apr. 2004.

[17] S. Tan, R. M. Narayanan, and S. K. Shetty, "Polarized lidar reflectance measurements of vegetation at near-infrared and green wavelengths," *Int. J. Infrared Millim. Waves*, vol. 26, no. 8, pp. 1175–1194, Jul. 2005.

[18] S. Kaasalainen, T. Lindroos, and J. Hyyppa, "Toward hyperspectral LiDAR: Measurement of spectral backscatter intensity with a supercontinuum laser source," *IEEE Geosci. Remote Sens. Lett.*, vol. 4, no. 2, pp. 211–215, Apr. 2007.

[19] S. Svanberg, "Fluorescence lidar monitoring of vegetation status," *Phys. Scr.*, vol. 1995, no. T58, pp. 79–85, 1995.

[20] F. Morsdorf, C. J. Nichol, T. J. Malthus, and I. H. Woodhouse, "Modelling multi-spectral LIDAR vegetation backscatter–assessing structural and physiological information content," *Remote Sens. Environ.*, vol. 113, no. 10, pp. 2152–2163, Oct. 2009.

[21] S. Jacquemoud and F. Baret, "Prospect—A model of leaf optical-properties spectra," *Remote Sens. Environ.*, vol. 34, no. 2, pp. 75–91, Nov. 1990.

[22] R. P. Leersnijder, "Pinogram a pine growth area model," *Ecological Model.*, vol. 61, no. 1/2, pp. 1–147, 1992, VI–XI.

[23] I. H. Woodhouse, Izzawati, E. D. Wallington, and D. Turner, "Edge effects on tree height retrieval using X-band interferometry," *IEEE Geosci. Remote Sens. Lett.*, vol. 3, no. 3, pp. 344–348, Jul. 2006.

[24] M. Disney, P. Lewis, and P. Saich, "3D modelling of forest canopy structure for remote sensing simulations in the optical and microwave domains," *Remote Sens. Environ.*, vol. 100, no. 1, pp. 114–132, Jan. 2006.

[25] B. Koetz, M. Schaepman, F. Morsdorf, K. Itten, and B. Allgöwer, "Radiative transfer modeling within a heterogeneous canopy for estimation of forest fire fuel properties remote sensing of environment," *Remote Sens. Environ.*, vol. 92, no. 3, pp. 332–344, Aug. 2004.